

where λ is the spin-orbit coupling constant (positive for less than half-filled shells). In deriving these relations, it is assumed that the lowest orbital level is non-degenerate, that there is no mixing of this level with higher orbital states and that spin-spin interactions within the ion can be neglected. From the g values given in Table I, these relations predict D positive and E negative in agreement with experiment. However, the magnitude of λ calculated from the equation for $2D$ is significantly larger than the free-ion value¹⁷ of $+92 \text{ cm}^{-1}$ in apparent disagreement with the decrease in λ usually

¹⁷ D. S. McClure, in *Solid State Physics*, edited by F. Seitz and D. Turnbull (Academic Press Inc., New York, 1959), Vol. IX, p. 428.

found^{18,18,19} in the crystal. This anomaly may indicate that the effect of configurational mixing or spin-spin interactions should be taken into account in the derivation of the equations for D and E given above.

ACKNOWLEDGMENTS

The authors wish to thank J. J. Rubin and L. G. Van Uiter for providing the zinc tungstate crystals, J. B. Mock and H. W. Reinbold for assistance in making the measurements and Mrs. W. L. Mammel for programming the energy level calculations. The authors also benefited from discussions with J. E. Geusic, E. O. Schulz-DuBois, H. E. D. Scovil, M. Peter, and S. Geller.

¹⁸ J. Owen, Proc. Roy. Soc. (London) **A227**, 183 (1955).

¹⁹ M. Tinkham, Proc. Roy. Soc. (London) **A236**, 549 (1956).

Paramagnetic Resonance and Charge Compensation of Tetravalent Uranium (U^{4+}) in Calcium, Strontium, and Barium Fluorides

AMNON YARIV

Bell Telephone Laboratories, Incorporated, Murray Hill, New Jersey

(Received June 12, 1962)

A new electron spin paramagnetic resonance spectrum in CaF_2 doped with uranium is attributed to U^{4+} . The spectrum possesses axial symmetry about the $\langle 111 \rangle$ directions and is describable by a spin Hamiltonian with $g_{\perp} = 0 \pm 0.15$ and $g_{\parallel} = 3.238 \pm 0.005$ at $4.2^\circ K$. The trigonal symmetry is due to the presence of charge compensating O^{2-} ions along the $\langle 111 \rangle$ directions. The spectrum is absent in crystals grown under reducing conditions. Similar results were also observed in SrF_2 and BaF_2 .

I. INTRODUCTION

PARAMAGNETIC resonance studies of uranium have been limited mostly to the trivalent ion.¹⁻³ Ghosh, Gordy, and Hill⁴ have reported a resonance in UF_4 ; unfortunately, the powder form of the sample and the high concentration made the interpretation difficult. Paramagnetic resonance on solid solutions of $ThO_2:U^{4+}$ has been observed by Llewellyn⁵ with $g \approx 2.7$. In this paper we report on a paramagnetic resonance spectrum observed in single crystals of CaF_2 doped with $\sim 0.1\%$ of uranium. After accounting for the resonance lines arising from U^{3+} ions in sites of fourfold symmetry¹ and lines due to U^{3+} ions in sites lacking axial symmetry, we are left with a set of lines possessing a threefold symmetry about the $\langle 111 \rangle$ cube diagonals. This spectrum is assigned to U^{4+} ions substituting for Ca^{++} ions. The extra positive charge ($+2e$) is believed to be com-

pensated by two O^{2-} ions replacing two F^- ions along any of the $\langle 111 \rangle$ directions, thus giving rise to the observed trigonal spectrum. The assignment of this spectrum to U^{4+} ion ($5f^2$) rather than U^{3+} ions ($5f^3$) is based on certain features of the paramagnetic resonance which can be explained if we assume a low-lying non-Kramer's doublet arising from an even number of electrons. This assignment is strengthened further by the dependence of the U^{4+} spectrum on the crystal growing conditions. The bulk of the investigation was devoted to CaF_2 host crystals. The presence of U^{4+} was detected also in SrF_2 and BaF_2 .

II. EXPERIMENTAL RESULTS

The ground state of tetravalent uranium is 3H_4 . The presence of compensating charges along the $\langle 111 \rangle$ directions, which is described in Sec. V, causes the local symmetry of the U^{4+} ion, which substitutes for a Ca^{++} ion, to be of the trigonal, C_{3v} , type. The ninefold degeneracy is split into

$$2A_1 + A_2 + 3E_1,$$

i.e., into three doublets and three singlets with one of the doublets lying lowest. The observed paramagnetic

¹ B. Bleaney, P. M. Llewellyn, and D. A. Jones, Proc. Phys. Soc. (London) **A69**, 858 (1956).

² G. Vincow and W. Low, Phys. Rev. **122**, 1390 (1961).

³ C. A. Hutchinson, Jr., P. M. Llewellyn, E. Wong, and B. P. Dorain, Phys. Rev. **102**, 292 (1956).

⁴ S. N. Ghosh, W. Gordy, and D. G. Hill, Phys. Rev. **96**, 36 (1954).

⁵ P. M. Llewellyn, thesis, Oxford, 1956 (unpublished).

resonance spectrum at low temperatures (<20°K) is due to transitions between the Zeeman split levels of the low-lying doublet. The eigenfunctions of this doublet, in perfect C_{3v} symmetry would be made up of an admixture of states with $J=4$ and $J_z=\pm 4, \pm 1, \mp 2$, which is such, as will be discussed in more detail in Sec. IV, that in addition to having $g_1=0$, which is usually the case for non-Kramer's doublets, $\langle \alpha | J_z | \beta \rangle$ is also zero and no transitions should be observed. The observed transitions are found to be due to the component of the microwave field which is parallel to the trigonal axis. This can be explained if we assume random local departures in the crystal from the perfect C_{3v} symmetry. These distortions will cause an additional admixture, most probably of the type $\Delta M = \pm 2$ which introduces the $|0\rangle$ wave function thus making possible $\Delta M = 0$ transitions.

For an arbitrary direction of the dc magnetic field, we find four lines which are due to charge compensation along each of the four $\langle 111 \rangle$ directions. These lines are fully consistent with a Hamiltonian

$$\mathcal{H} = g_{11}\beta S_z H_z + \Delta_x S_x + \Delta_y S_y, \quad (1)$$

where β is the Bohr magneton. S_z , S_x , and S_y are the components of the effective spin vector \mathbf{S} with $S = \frac{1}{2}$. H_z is the projection of the dc magnetic field along the "z" direction which is the direction of the trigonal axis. g_{11} is the component of the g tensor along the trigonal field axis. Δ_x and Δ_y represent the departure from axial symmetry.⁶ Within the framework of the effective spin Hamiltonian, the terms $\Delta_x S_x$ and $\Delta_y S_y$ in Eq. (1) cause a $\Delta S_z = \pm 1$ admixture, thus making possible $\Delta S_z = 0$ transitions when the rf magnetic field \mathbf{H}_1 has a z component.

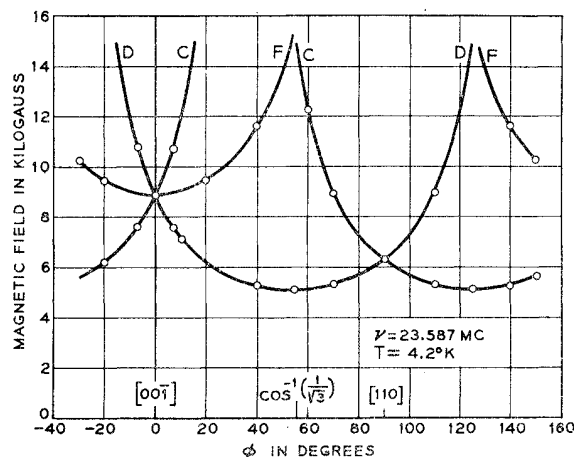


FIG. 1. Variation of the resonance magnetic field for the trigonal sites as a function of the angle between the magnetic field and the trigonal axis. The magnetic field is in the (110) plane. The solid curve is based on Eq. (2) with $\Delta=0$ and $g_{11}=3.238$. The circles are experimental points.

⁶ B. Bleaney, P. M. Llewellyn, M. H. L. Pryce, and G. R. Hall, Phil. Mag. 45, 991 (1954).

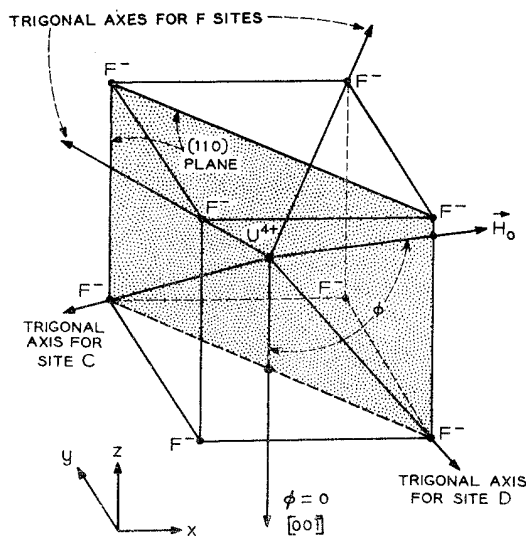


FIG. 2. The location of the four trigonal axes in relation to the cubic structure and the magnetic field. The direction of each vector can be ascertained from the position of the two black dots. The (110) plane is dotted.

Diagonalization of Eq. (1) yields

$$H = \frac{[(\hbar\omega)^2 - \Delta^2]^{1/2}}{g_{11}\beta \cos\theta}, \quad (2)$$

where $\Delta^2 = \Delta_x^2 + \Delta_y^2$, θ is the angle between the applied dc magnetic field \mathbf{H} and the trigonal field (z) axis.

Assuming the distortion parameter Δ^2 to have a random symmetric distribution about some mean value and recognizing that the strength of the transition for a spin packet characterized by a given Δ^2 is proportional to Δ^2 , it follows that spins with a high value of Δ^2 absorb more energy than the same number of spins with a lower value of Δ^2 . This fact, coupled with the dependence of H on Δ^2 [Eq. (2)], leads to the observed asymmetric line shape with its steep drop on the high-field side as exemplified by line C in Fig. 3. To obtain g_{11} , the dc magnetic field was measured at the base of the absorption line on the high-field side, where $\Delta=0$, at $\theta=0^\circ$. The result is

$$|g_{11}| = 3.238 \pm 0.005 \text{ at } 4.2^\circ\text{K.}$$

The rms value of Δ was estimated by assuming a Gaussian distribution for (Δ^2) ,⁶

$$\langle \Delta^2 \rangle^{1/2} \sim 2 \times 10^{17} \text{ cgs} \sim 0.1 \text{ cm}^{-1}.$$

Since the highest magnetic field available in this experiment was $\sim 15\,000$ G, our estimate of g_1 was not based on a direct measurement but rather on the fit between the experimental resonance data and the general ($g_1 \neq 0$) form of Eq. (2)

$$H = \frac{[(\hbar\omega)^2 - \Delta^2]^{1/2}}{\beta [g_{11}^2 \cos^2\theta + g_1 \sin^2\theta]^{1/2}}, \quad (3)$$

The result is

$$g_1 = 0 \pm 0.15.$$

Figure 1 shows the variation of the observed magnetic field H as a function of the angle φ between the applied magnetic field and the $[00\bar{1}]$ axis. With the magnetic field applied in the (110) plane, two of the four trigonal lines are due to sites whose axes lie in the (110) plane at 54.76° and -54.76° [$\pm \cos^{-1}(1/\sqrt{3})$] with respect to the $[00\bar{1}]$ direction. The spectra of these sites are labeled D and C , respectively. The remaining two trigonal sites are equivalent and give rise to a single line which is labeled, in Fig. 1, as F . The position of the four trigonal sites in relation to the basic cubic cell containing the uranium ion is shown in Fig. 2.

The angle θ , between the applied magnetic field and each of the four trigonal axes, is given by

$$\begin{aligned} \theta_C &= \varphi + \cos^{-1}(1/\sqrt{3}) = \varphi + 54.76^\circ, \\ \theta_D &= \varphi - \cos^{-1}(1/\sqrt{3}) = \varphi - 54.76^\circ, \\ \theta_F &= \cos^{-1}((\cos \varphi)/\sqrt{3}), \end{aligned} \quad (3)$$

where φ is the angle between the magnetic field vector and the $[00\bar{1}]$ direction.

The solid curves of Fig. 1 were obtained by using Eq. (2) with $|g_{11}| = 3.238$, $\Delta = 0$ and the respective values of θ as given by Eqs. (3). When $\varphi = 0^\circ$, i.e., when the applied magnetic field is parallel to one of the cube edges, we have

$$|\theta_C| = |\theta_D| = |\theta_F| = \cos^{-1}(1/\sqrt{3}),$$

and the three spectra coincide. The extrema of each of the three spectra occur at the maxima and minima of $|\cos \theta|$ as given by Eq. (3). This constitutes sufficient proof for the trigonal symmetry of the sites.

Small deviations from perfect alignment of the crystal will spoil the perfect equivalence of the two sites which give rise to spectrum F and the latter appears as a doublet. The doublet separation is zero at $\varphi = 0$ and increases as φ is increased from zero toward 90° . The

experimental points in Fig. 1 are those of the center of gravity of the doublet.

Figure 3 shows an absorption run taken at $\varphi = 40^\circ$. No field modulation is employed so that the ordinate is proportional to $\chi'' H_{1z}$. Only line C and the doublet F are present at this orientation. Line D occurs at a value of H which is outside our reach. The crystal orientation is such that the rf magnetic field is nearly perpendicular to the trigonal axes of sites C and D , a fact which explains the relative weakness of their absorption as compared to that of the two F sites.

The lines labeled as A and B arise from the tetragonal U^{3+} sites discussed by Bleaney *et al.*¹ The compensation axis for the site giving rise to line B is the $[001]$ direction and is contained, along with the magnetic field, in the (110) plane. The sites with axes along the (010) and $[100]$ directions are magnetically equivalent when \bar{H} is in the (110) plane and give rise to line A . Small deviations from perfect alignment will split this line into a doublet. The remaining lines, X_1 , X_2 , X_3 , X_4 , and Y , belong to yet another site discussed separately in Sec. VI. Since all the crystals investigated had a considerable fraction (ranging from 0.1 to 0.99) of tetragonal sites, we are including in Fig. 4 a plot of the resonance magnetic field for these sites as a function of φ under experimental conditions identical to those specified for Fig. 1. The data of Fig. 4 can be fitted with $|\pm g_{11}| = 3.528 \pm 0.005$ and $|g_1| = 1.875 \pm 0.005$. The small discrepancy between these values and those reported by Bleaney *et al.*¹ could be due to the fact that our data were obtained at 4.2°K while theirs were obtained at 20°K .

III. EXPERIMENTAL NOTES

The experiments were conducted at 4.2°K . Strong resonance signals were also observed at 20°K but not at 78°K . This is probably due to short thermal relaxation time at the latter temperature. The paramagnetic resonance spectrometer was of the superheterodyne type, with an intermediate frequency of 60 Mc/sec, capable of covering the 21–24 kMc/sec range. The signal and

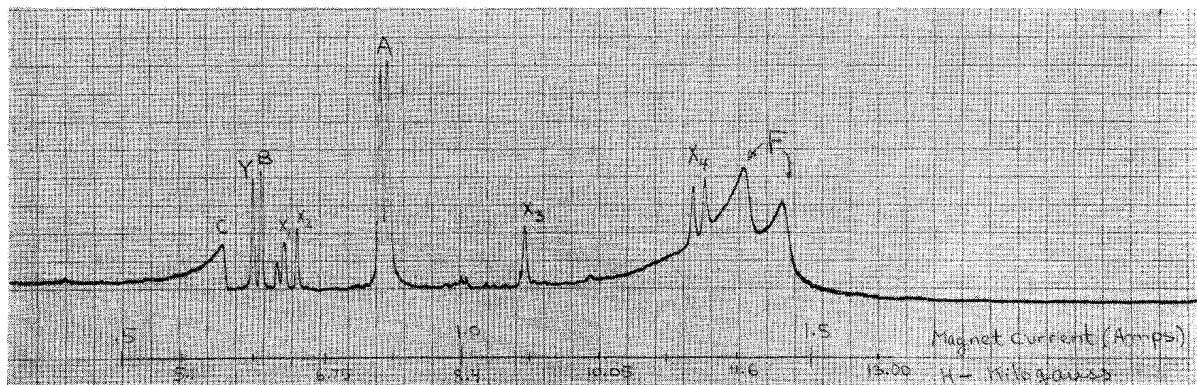


FIG. 3. Actual absorption run at $\varphi = 40^\circ$. The ordinate is proportional to $\chi'' H_{1z}$. The abscissa is marked by the magnetic field values.

local oscillator power were provided by two stabilized 2K33 klystrons. The sample cavity operated in the TE₀₁₁ mode with the sample placed at its center. The sample and cavity orientation were such that the rf magnetic field at the sample position was always perpendicular to the dc magnetic field.

The coupling of the cavity as well as the sensitivity of the receiver to χ'' or χ' were controlled by a variable-coupling scheme which was previously described by Gordon.⁷ The precision measurements of the magnetic field were performed by a nuclear magnetic resonance probe and frequency counters. The rf frequency was determined by measuring the beat frequency obtained by mixing the signal power with a known harmonic of a quartz crystal stabilized 20-Mc/sec oscillator. The crystals were oriented with the aid of an x-ray goniometer.

Magnetic fields of up to 15 kG were provided by a 12-in. Varian magnet rotatable about a vertical axis. Linear sweep of the magnetic field was provided by the use of a function generator. Sinusoidal sweep of up to 50-G peak amplitude and at frequencies of up to 100 cps was used when phase sensitive detection was employed and was provided by Helmholtz coils wound around the pole faces.

IV. THEORY

The crystalline electric field at the site of the uranium ion possesses a threefold C_{3v} symmetry. The electric field can be expanded in terms of the generalized Legendre polynomials $Y_m^n(\theta, \varphi)$. Since we are dealing with a $5f$ configuration, only terms with $n \leq 6$ yield nonzero matrix elements. The terms with odd n are omitted because of parity considerations.⁸ The perturbation Hamiltonian has the form⁹

$$V = A_0^2 Y_0^2 + A_0^4 Y_0^4 + A_3^4 (Y_3^4 + Y_{-3}^4) + A_0^6 Y_0^6 + A_3^6 (Y_3^6 + Y_{-3}^6) + A_6^6 (Y_6^6 + Y_{-6}^6). \quad (4)$$

The ninefold degeneracy of the ${}^3H_4(5f^2)$ ground state can be shown by group-theoretical methods to be split into three doublets and three singlets. The observed absorption is due to transitions between the Zeeman split levels of the lowest doublet. The wave functions for the doublet are made up of linear combinations of the $J=4$ manifold wave functions. If the linear combination is dominated by a single member $|M\rangle$ we expect the relation

$$g_{11} \sim 2\Delta M$$

to hold, where Δ is the Lande- g factor. For 3H_4 $\Delta = 0.8$ and since $g_{11} = 3.238$, $M = 2$. The wave functions of the

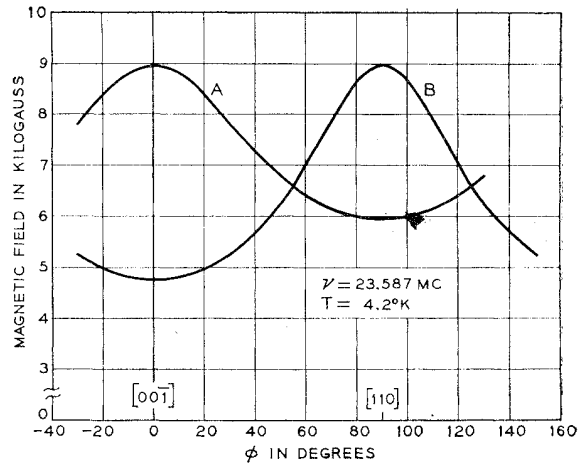


FIG. 4. The resonance magnetic field for the tetragonal sites of U^{3+} as a function of the angle between the magnetic field and the $[00\bar{1}]$ direction. The magnetic field is in the (110) plane.

doublet are thus dominated by $|2\rangle$ and $|-2\rangle$. Since admixture of $\Delta M = \pm 3, \pm 6$ is allowed by the perturbation Hamiltonian for C_{3v} symmetry [Eq. (4)]. The total wave functions can be written as¹⁰

$$\begin{aligned} |\alpha\rangle &= a|4\rangle + b|1\rangle + c|-2\rangle, \\ |\beta\rangle &= a|-4\rangle - b|-1\rangle + c|2\rangle, \end{aligned} \quad (5)$$

where $a < c$ and $b < c$. The minus sign preceding the $|-1\rangle$ ket is necessary in order to make

$$g_1 = 2\langle\alpha|L_x + 2S_x|\beta\rangle = 0.$$

The paramagnetic resonance data are not sufficient to solve for a, b, c . We can only write two equations:

$$a^2 + b^2 + c^2 = 1,$$

which is the normalization condition and

$$g_{11} = 2\langle\beta|J_z|\beta\rangle = 4a^2 + b^2 - 2c^2 = 3.238$$

for the three unknowns a, b , and c . To solve for a, b , and c , it is necessary to use optical absorption data in order to evaluate the "A" parameters in the spin Hamiltonian. We have neglected the added admixture from the 3H_5 level.

As mentioned earlier, the matrix element, $\langle\alpha|J_z|\beta\rangle$ is zero when $|\alpha\rangle$ and $|\beta\rangle$ are given by Eq. (5). The effectiveness of the "z" component of the rf magnetic field in inducing transitions is attributed to further admixture, caused by local departures from C_{3v} symmetry, which makes possible $\Delta M = 0$ transitions. This assumption is corroborated by the asymmetric resonance line shape as discussed in Sec. II.

V. THE CHARGE COMPENSATION

The replacement of an ion belonging to the host crystal by an impurity ion with a different net charge,

⁷ J. P. Gordon, Rev. Instr. **32**, 658 (1961).

⁸ W. Low, *Paramagnetic Resonance in Solids* (Academic Press Inc., New York, 1960), p. 12.

⁹ R. J. Elliot and K. W. H. Stevens, Proc. Roy. Soc. (London) **A215**, 437 (1952).

¹⁰ B. R. Judd, Proc. Roy. Soc. (London) **A232**, 458 (1955).

requires charge compensation to restore the electrostatic charge neutrality. The crystal structure of CaF_2 is O_h^5 which can be described as a cubic lattice of F^- ions with Ca^{++} ions at every other body center. Thus each uranium ion, substituting for a Ca^{++} , is at the center of a cube of eight F^- ions. The tetragonal spectrum of U^{3+} in CaF_2 was explained by Bleaney *et al.*¹ as being due to an interstitial F^- ion occupying the otherwise vacant center of nearest cube along any of the $\langle 100 \rangle$ axes. The possibility of charge compensation via the replacement of one of the nearest F^- ions by an O^{2-} ion was suggested by Feofilov and Stepanov.^{11,12} This scheme gives rise to spectra possessing threefold symmetry about the $\langle 111 \rangle$ directions. Experimental verification for this compensation scheme in $\text{CaF}_2:\text{Gd}^{3+}$ was provided by Sierro.¹³ Additional confirmation for the existence of this mechanism was provided by the work of Forrester and Hempstead¹⁴ on $\text{CaF}_2:\text{Tb}^{3+}$. Cubic sites in $\text{CaF}_2:\text{U}^{3+}$ were described by Vincow and Low.² In the case of $\text{CaF}_2:\text{U}^{4+}$ the excess $+2e$ charge, introduced into the lattice when a U^{4+} ion replaces a Ca^{++} , has to be compensated. This can take place by having two F^- ions which are on opposite sides of the U^{4+} ion along the cube diagonal, replaced by O_2^- ions. A second mechanism, less likely but one we could not rule out, involves the occupation of the first cube center (normally vacant) along any of the $\langle 111 \rangle$ directions by an O_2^- ion.

Partial confirmation for the validity of the mechanism proposed above was provided by the dependence of the concentration of U^{4+} on the crystal-growing conditions. The crystals were grown by W. A. Hargreaves of Optovac Inc., using the Stockbarger-Bridgeman method in which a graphite crucible containing molten CaF_2 and uranium was gradually lowered through a heating induction coil. If the crucible and the melt were kept at $\sim 100^\circ\text{C}$ above the melting temperature for ~ 2 h before cooling, no trace of U^{4+} was found in the crystal. This is probably due to the reduction action of the graphite crucible. The compensation mechanism postulated above depends on the presence of oxygen in the melt. If the oxygen is removed by the carbon, compensation cannot take place and the uranium enters the crystal as U^{3+} in tetragonal sites and the compensation is achieved by interstitial F^- ions.

It may be of interest to note in this connection that the present investigation arose from an effort to lower

the threshold for optical maser action in $\text{CaF}_2:\text{U}^{3+}$ and that only after the complete elimination of the U^{4+} ions did the threshold become low enough so that continuous operation, rather than pulsed was achieved.¹⁵

VI. NONAXIAL SITES

In the course of this investigation we found, in addition to the tetragonal U^{3+} and the trigonal U^{4+} spectra, an additional group of lines shown in Fig. 3 as X_1 , X_2 , X_3 , and Y . The optical spectrum of the sites giving rise to these lines occupies the same general spectral region as that of the $\text{CaF}_2:\text{U}^{3+}$ tetragonal sites. The lines are consequently believed to arise from U^{3+} ions in a new site which lacks an axis of symmetry and which gets its charge compensation from F^- ions in the next nearest interstitial cube center. Fuller details on these sites will be given in a separate paper.

We have referred to the trigonal spectrum on two previous occasions^{15,16} as being due to U^{3+} . This assignment, as made evident by the present paper, was in error and should be corrected to $\text{CaF}_2:\text{U}^{4+}$.

VII. RESONANCE IN $\text{SrF}_2:\text{U}^{4+}$ AND $\text{BaF}_2:\text{U}^{4+}$

Trigonal spectra attributed to U^{4+} were also observed in SrF_2 and BaF_2 doped with uranium. Due to the large amount of strain in the crystals, the lines were very broad which decreased the accuracy with which the spin Hamiltonian parameters could be determined. These parameters are:

$$\begin{aligned} \text{SrF}_2:\text{U}^{4+} & \quad g_{11} = 2.85 \pm 0.05, g_{\perp} \sim 0, \quad \text{at } 4.2^\circ\text{K}; \\ \text{BaF}_2:\text{U}_4^{4+} & \quad g_{11} \sim 3, g_{\perp} \sim 0, \quad \text{at } 4.2^\circ\text{K}. \end{aligned}$$

A brief account of this work was given by the author at the First International Conference on Paramagnetic Resonance, Jerusalem, Israel, July, 1962.

ACKNOWLEDGMENTS

It is a pleasure to acknowledge the extremely helpful communication with Professor B. Bleaney who first suggested the possibility of the U^{4+} spectrum. W. A. Hargreaves of "Optovac Inc.," provided the many crystals investigated and was instrumental in establishing the correlation between the growing conditions and the U^{4+} concentration. We have also benefited from many discussions with Dr. J. P. Gordon and from the able experimental assistance of J. M. Dziedzic.

^{11a} P. P. Feofilov, J. phys. radium **17**, 656 (1956).

^{11b} P. P. Feofilov, Doklady Akad. Nauk. USSR **99**, 731 (1954).

¹² I. V. Stepanov and P. P. Feofilov, Soviet Phys.—Doklady **1**, 350 (1956).

¹³ Jerome Sierro, J. Chem. Phys. **34**, 2183 (1961).

¹⁴ P. A. Forrester and C. F. Hempstead, Phys. Rev. **126**, 923 (1962).

¹⁵ G. D. Boyd, R. J. Collins, S. P. S. Porto, and W. A. Hargreaves, Phys. Rev. Letters **8**, 269 (1962).

¹⁶ S. P. S. Porto and A. Yariv, J. Appl. Phys. **33**, 1620 (1962).

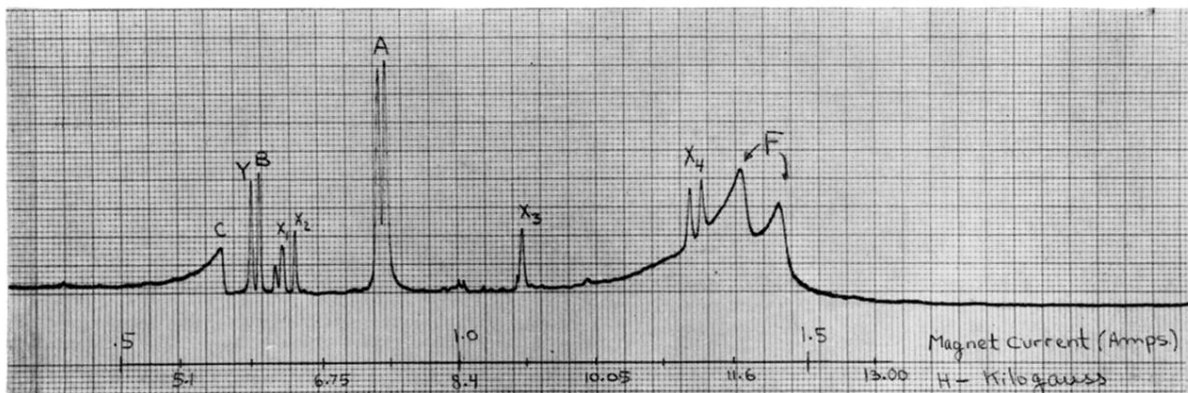


FIG. 3. Actual absorption run at $\varphi=40^\circ$. The ordinate is proportional to $\chi'' H_{1z}$. The abscissa is marked by the magnetic field values.